PAPER • OPEN ACCESS

Rheological modelling of viscoelastic fluid in a generic gap of screw pump

To cite this article: S Mehrnia *et al* 2022 *IOP Conf. Ser.: Mater. Sci. Eng.* **1267** 012013

Rheological modelling of viscoelastic fluid in a generic gap of screw pump

S Mehrnia, L Kerres, M Kuhr and P F Pelz

Chair of Fluid Systems, Technische Universität Darmstadt, Otto-Berndt-Straße 2, 64287 Darmstadt, Germany

E-mail: seyedmajid.Mehrnia@fst.tu-darmstadt.de

Abstract. In this study, the leakage of a non-Newtonian fluid, i.e. silicone oil, in a generic gap was numerically investigated. A CFD tool is used to determine the relationship between leakage flow, gap length and pressure difference. The investigated fluid is viscoelastic and its properties are modelled by a Maxwell equation. The Maxwell model can be used to precisely define the phenomenon of stress relaxation. Moreover, a comparison of the viscosity of measured data with simplified models shows that the Maxwell model is best suited for viscosity prediction. Furthermore, simulation results showed that at low pressures, leakage is reduced by decreasing the gap angle. However, this effect changes with increasing viscosity and relaxation time of the molecule. To determine the pressure drop, the Bagley plot is used. The results confirmed that as the shear rate increases, the elastic pressure drop values increase. In addition, the leakage flow increases with an increasing slenderness ratio.

1. Introduction

The effect of viscoelasticity on lubrication properties has recently become more important due to the effect of lubricant viscosity on energy efficiency. Thus, there are good practical reasons to investigate the general issue of viscoelastic effects in the narrow gaps of screw pumps. Due to their design, leakage occurs inside the pumps, between the rotating and non-rotating parts. Therefore, several experimental, analytical and numerical investigations have been carried out to understand the behaviour of leakage and to describe the flow of Newtonian fluids through these gaps. Rituraj et al. [1-3] modelled and experimentally validated gap losses for a generic gap in positive displacement pumps. Türk et al. [4] experimentally investigated the leakage behaviour of lobe pumps by measuring the volume flow through a blocked pump. Various influencing parameters such as geometry and pressure difference on the leakage were investigated for several pump types by calculating the leakage volume flow [5, 6]. Besides, also analytical and numerical studies have been carried out. It is common to model external gear pumps by using modes ranging from "lumped parameter" (0D) to Computational Fluid Dynamics (3D), cf. Rundo [7]. Those studies aimed to predict the leakage behaviour of the pumps.

It has been shown that there are several investigations on Newtonian fluids, but the literature dealing with non-Newtonian fluids in narrow gaps is scarce. Nevertheless, rotary positive displacement pumps are used daily to convey non-Newtonian viscoelastic fluids like plastic, paints, inks etc. For gear pumps, Rituraj et al. [8] extended an existing modell describing the displacement action of the unit to investigate the behaviour of leakage for non-Newtonian fluids. Rothstein et al. [9] showed that the influence of the inlet geometry on the behaviour of non-Newtonian fluids is crucial. Depending on the type of rotary displacement pump this geometry can strongly vary. Screw pumps, which have complex geometry are hardly researched. Furthermore, it can be shown that the tooth side gap has a major impact on the leakage behaviour, i.e. the efficiency. Hence, this paper aims to systematically analyse the leakage behaviour of non-Newtonian fluid within the generic gap pictured in Figure 1.

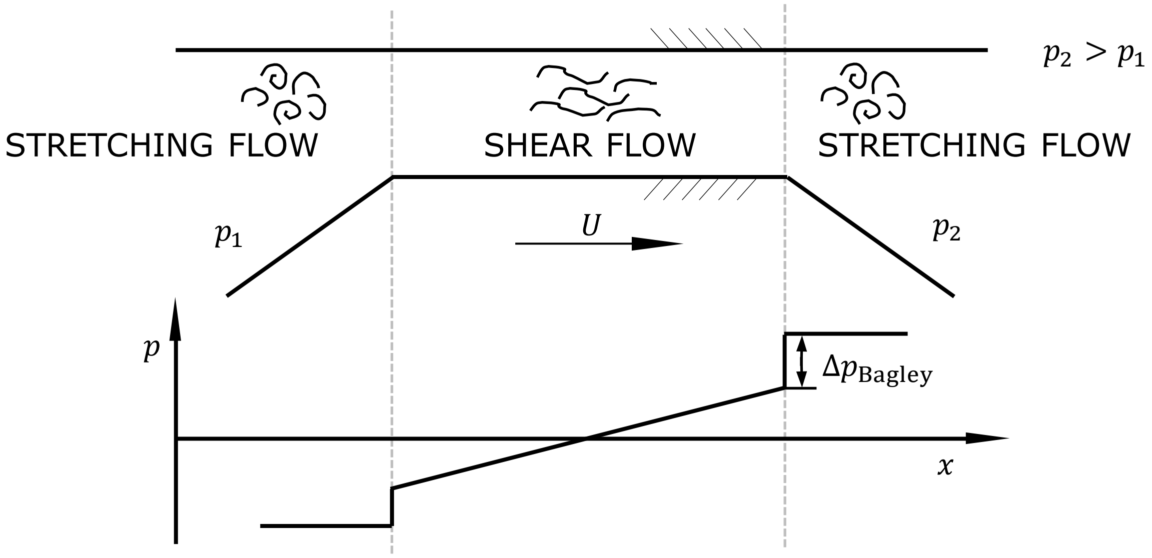

Figure 1. Generic gap inside a positive displacement pump including the stretches exerted on the fluid as well as the pressure in the narrow gap.

Within this paper, the leakage flow in the clearance gap between a stationary and a moving wall is investigated numerically by using Computational Fluid Dynamics (CFD) to find the relationship between leakage flow, gap length, and pressure difference. This work aims to predict the leakage flow rate in a generic gap of a screw pump. Figure 1 shows a schematic view of a generic gap as well as the pressure and the stretches exerted on the viscoelastic fluid. Here, the molecules of the fluid are stretched when entering and relaxed when exiting the gap. The stretching of the molecules leads to an elastic pressure loss in the inflow, i.e. the Bagley pressure loss, which is significant at high molecular mass liquids.

2. Methodology

Focussing on the generic gap, the flow inside is depending on eight parameters, cf. Figure 2.

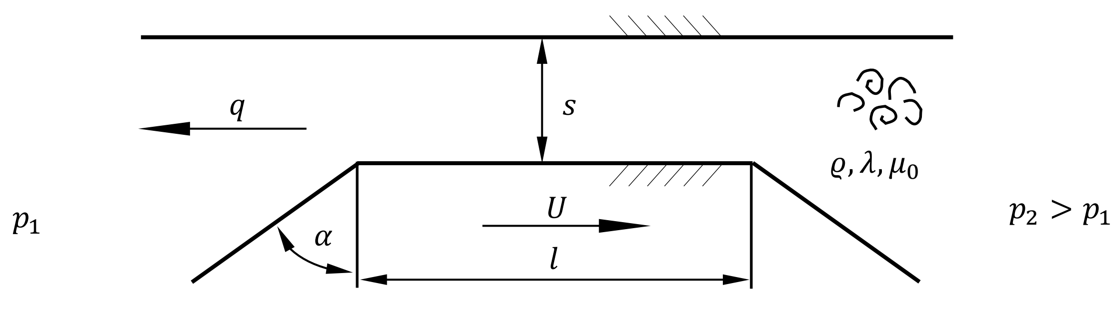

Figure 2. Schematic view of the generic gap and its parameters.

Here, s is the gap clearance, μ_0 is the constant viscosity of a Newtonian fluid, Δp is the pressure difference across the gap $\Delta p = p_2 - p_1$, q is the leakage flow rate (volume flow per width), ϱ is the density of the fluid, λ is the relaxation time of the molecules, U is the velocity of the moving wall, and

IOP Conf. Series: Materials Science and Engineering 1267 (2022) 012013 doi:10.1088/1757-899X/1267/1/012013

T is the characteristic process time. The viscoelastic flow is modelled using the commercial finite element software ANSYS POLYFLOW. The continuity and momentum equations are solved for the incompressible viscous flow field of the continuous phase. The flow is assumed to be stationary and the temperature is assumed to be constant. The fluid under consideration is a non-Newtonian viscoelastic fluid modelled by a Maxwell constitutive equation, cf. section 2.2. Two different molecular masses 10,000 and 20,000 u were simulated. Also, the simulations were carried out at two different gap heights $s = 20$ and 50 µm. The gap length was varied to represent five different slenderness rations s/l ranging from $s/l = 0.02$ to 0.1.

To model the flow in the generic gap a structured grid with approximately 12800 cells was generated by layering cross-sections perpendicular to the axial direction. The results are represented in dimensionless forms by the dimensionless pressure difference Δp^+, the dimensionless leakage flow rate q^+ and the Deborah number De

$$\Delta p^+ \coloneqq \Delta p \frac{s^2 \varrho}{\mu_0^2}, \quad q^+ \coloneqq \frac{q\varrho}{\mu_0}, \quad De \coloneqq \frac{\lambda}{T} = \frac{\lambda U}{s} = \lambda\dot{\gamma}. \tag{1}$$

2.1. Non-Newtonian fluid

Unlike a Newtonian fluid, the viscosity of a non-Newtonian fluid is not constant. When sheared, the viscosity decreases or increases, depending on the type of fluid. This is due to the molecular chain structure of the liquid, which is one of the most characteristic features of non-Newtonian fluids. In some fluids, the molecules tend to orient to surfaces of maximum tension, causing the viscosity to decrease as the velocity gradient increases. These fluids are called shear-thinning fluids, meaning that the fluid becomes thinner as the shear rate increases. In other cases, the fluid is shear-thickening if the viscosity increases with an increasing velocity gradient. Therefore, the Newtonian model, i.e. modelling the liquid with a constant viscosity, is not applicable. The relationship between shear stress and shear rate can be represented as a power law for a viscous fluid:

$$\tau = m\dot{\gamma}^n. \tag{2}$$

Here, τ is the shear stress, $\dot{\gamma}$ is the shear rate, m is the flow consistency index, and n is the power-law index:

$n > 1$ fluid is shear-thickening,
$n = 1$ fluid is Newtonian,
$n < 1$ fluid is shear-thinning.

The shear-thinning behaviour of the fluid is described in terms of a relaxation time λ, defined by the ratio μ_0/G_0 of zero viscosity μ_0 and shear modulus G_0. The shear modulus is defined by the ratio between shear stress τ and shear strain γ, i.e. $G = \tau/\gamma$. Figure 3 shows the shear stress behaviour of a shear-thinning fluid in the function of shear rate. In fact, the relaxation time λ is equal to the inverse of the critical shear rate $1/\dot{\gamma}_0$.

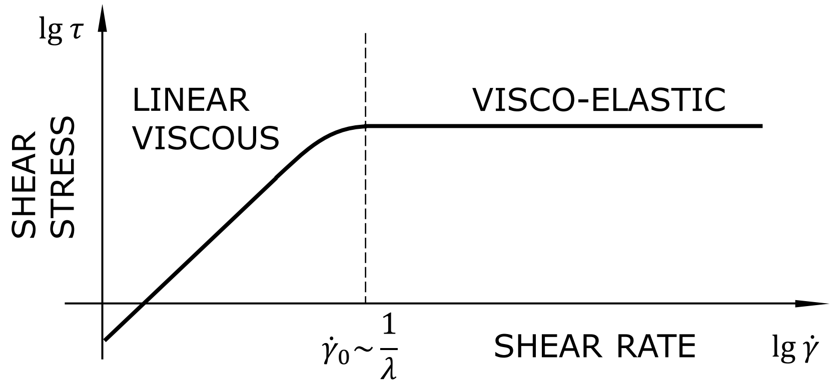

Figure 3. Shear stress behaviour of a shear-thinning fluid in the function of shear rate

In addition, polymeric liquids are viscoelastic, which means that the stress carried by a liquid component depends on the deformation history of this element. This effect is called the memory effect of polymeric fluids. These two nonlinearity and memory effects are responsible for considerable industry-related flow phenomena that must be predicted and controlled using a combination of mathematical and physical models.
We can divide non-Newtonian simulation models into two distinct groups. Some common models used in simulations are more of a fitting method, such as power-law and Carreau, which are called simplified models. Another class of viscoelastic fluid models with whole-order derivatives that have the locality property includes the Maxwell, Oldroyd-B, Kelvin-Voigt, Jeffreys, and Burgers models, which are called differential viscoelastic models. There are several internal variables or inputs for these models. The Maxwell equation is simple and shows less instability at the beginning of the simulation than other differential viscoelastic models. Table 1 has shown the differences between various viscoelastic models.

Table 1. Viscometric fluid functions.

Model	viscous shear stress	viscoelastic normal stress difference
Newton	$\tau = \mu_0 \, \dot{\gamma}$	no elastic effects
Prandl-Eyring	$\tau = \mu_0 \, \dot{\gamma} \frac{\operatorname{arsinh}(\lambda\dot{\gamma})}{\lambda\dot{\gamma}}$	$\sigma_i - \sigma_j = 0$
Power-Law	$\tau = m \, \dot{\gamma}^n$	$\sigma_i - \sigma_j = 0$
Carreau	$\tau = \mu_0 \, \dot{\gamma} \, [1 + (\lambda\dot{\gamma})^2]^{(n-1)/2}$	$\sigma_i - \sigma_j = 0$
Maxwell	$\tau = \mu_0 \, \dot{\gamma} \frac{1}{\sqrt{1+(\lambda\dot{\gamma})^2}}$	$\sigma_i - \sigma_j \approx \frac{1}{2} \mu_0 \, \lambda \, \dot{\gamma}^2$

2.2. Maxwell model
One of the simple viscoelastic models is the upper convected Maxwell model, including a constant viscosity and a relaxation time. Maxwell model represents the physical properties of the fluid with a mechanical analogue, in terms of a damper and a spring, which can accurately define the phenomenon of stress relaxation, cf. figure 4. In this arrangement, under applied axial stress, the total stress and strain can be represented as the stress-strain relation by equation (3):

$$\tau + \lambda \, \dot{\tau} = \mu_0 \, \dot{\varepsilon}. \tag{3}$$

where λ is relaxation time, μ_0 is zero shear viscosity, $\dot{\varepsilon}(t)$ is the rate of deformation tensor, and $\dot{\tau}(t)$ is upper convected derivative, cf. Li et al. [10]. Input values of the Maxwell model are the zero viscosity μ_0 and the relaxation time of the molecule λ. On the one hand, the equation of the Maxwell model is simple and shows less instability at the start of the simulation. On the other hand, however, the model is complicated from a computational point of view and is only recommended when little knowledge about the liquid is available.

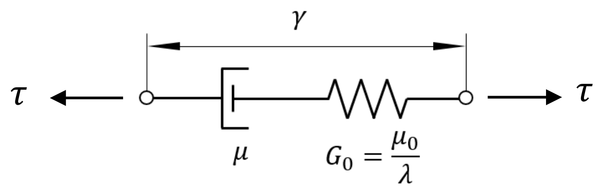

Figure 4. Mechanical analogue of the Maxwell model.

3. Measurement data analysis

The PhD thesis of Andrä [11] was used for the assumption of the measured rheological data and the derivation of the required viscosity from the storage and loss modulus curves G' and G'' given in his work. Andrä [11] has conducted extensive research for silicone oil with a large number of measurements in the selected temperature, molecular mass and shear rate range from a tribological point of view. The authors of this paper have judged the viscosity, storage and loss modulus results with the applied rheological methods in Andrä's work [11] to be reliable, accurate and well studied. The data of the storage and the loss moduli as a function of angular frequency were recorded during the measurements and are shown in figures 5 and 6.

The values of the complex G^* moduli as a function of the angular frequency Ω can be calculated using the storage moduli G' and the loss moduli G'' as a function of angular frequency Ω according to equation (4). Figures 7 and 8 show the master curve of the storage and the loss modulus of silicone oil. The dynamic viscosity μ as a function of shear rate $\dot{\gamma}$ can be derived from the absolute value of the μ^* complex dynamic viscosity data based on the Cox-Merz rule, cf. equation (7) [11]. The Cox–Merz rule is a simple relationship that signifies that complex viscosity and shear viscosity are comparable when the steady shear rate is the same as angular frequency.

$$|\mu^*(\Omega)| = \frac{|G^*|}{\Omega} = \frac{\sqrt{G'^2 + G''^2}}{\Omega} \tag{4}$$

$$G' = \frac{\mu}{\lambda} \frac{(\lambda\Omega)^2}{1 + (\lambda\Omega)^2} \tag{5}$$

$$G'' = \frac{\mu}{\lambda} \frac{\lambda\Omega}{1 + (\lambda\Omega)^2} \tag{6}$$

$$|\mu^*(\Omega)| = \mu\,(\dot{\gamma}) \;\;:\;\; \Omega = \dot{\gamma} \tag{7}$$

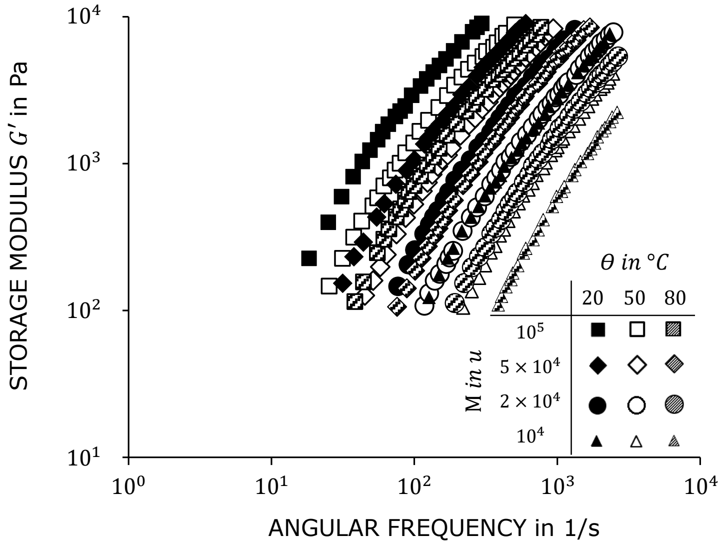

Figure 5. Measured values of storage modulus of silicone oil for different temperatures and molecular masses [11].

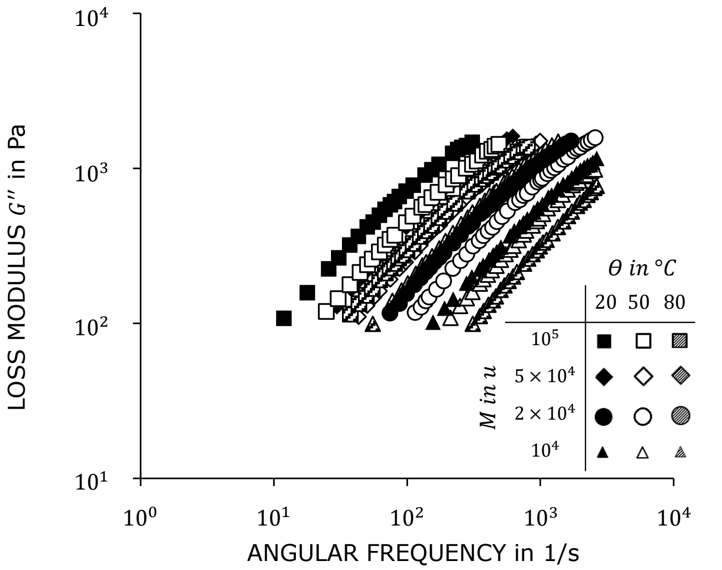

Figure 6. Measured values of loss modulus of silicone oil for different temperatures and molecular masses [11].

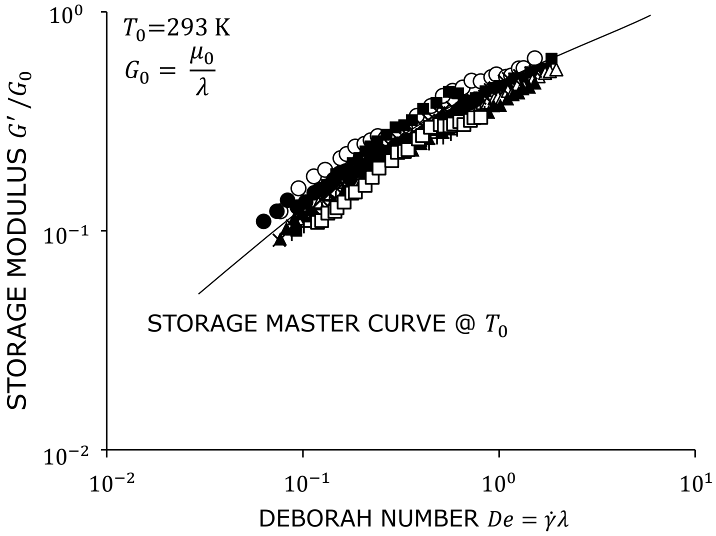

Figure 7. Storage modulus master curve for silicone oil.

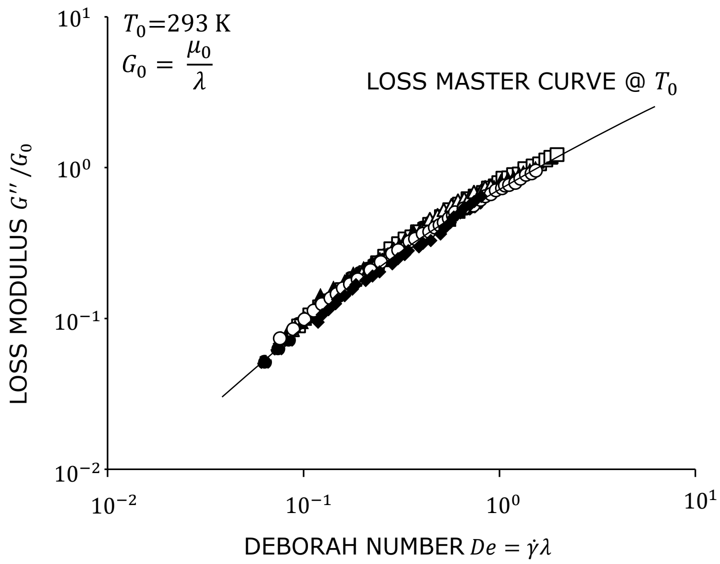

Figure 8. Loss modulus master curve for silicone oil.

Figure 9 shows a comparison of the dimensionless viscosity of measured data with different viscoelastic models. As it was explained, it can be seen that the Maxwell model is best suited for viscosity prediction. It is also evident that the other, simplified models are lacking in the reliable prediction of non-Newtonian behaviour. Here, for the Carreau model, the best power law index to fit the measurement data is $n = 0.3$.

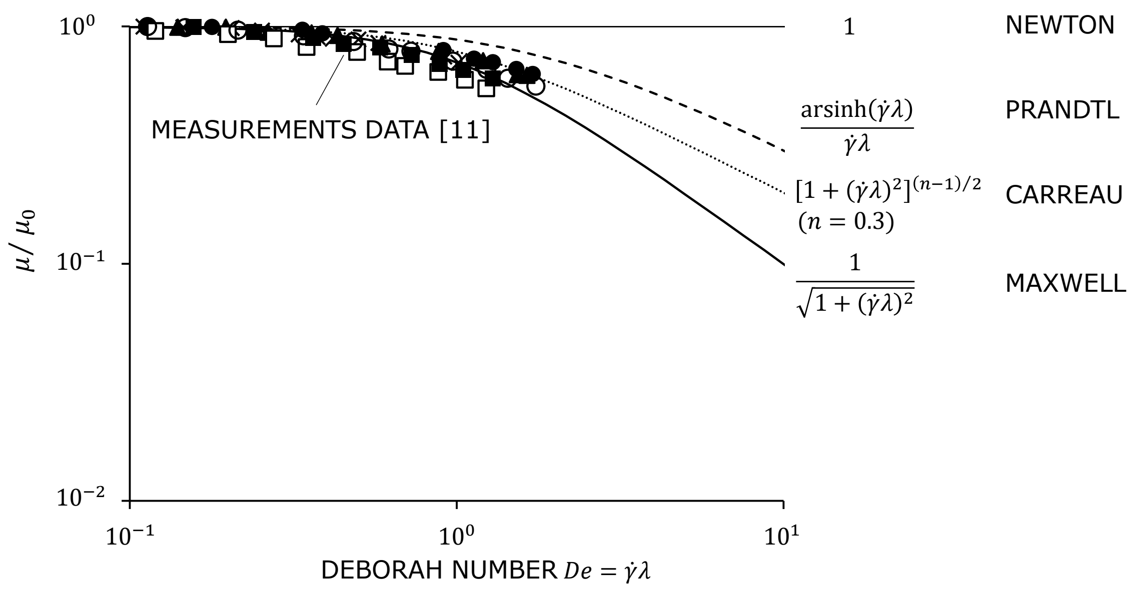

Figure 9. Comparison of dimensionless viscosity of measurement data with different viscoelastic models.

3.1. Relaxation time

The relaxation time of a molecule λ is a function of molecular mass and temperature. In viscoelastic modelling by Maxwell, the zero viscosity μ_0 and relaxation time λ are inputs for the simulation. Hence, it is necessary to calculate the relaxation time of silicone oil from the measurement data. Equation (5) was employed to calculate the relaxation time. Figure 10 has shown Arrhenius plot for the relaxation time of silicone oil molecules in various molecular masses. As it can be seen, the logarithmic ratio of relaxation time is a linear function of the inverse temperature, called the Arrhenius law. However, at high molecular mass, the variations are non-linear.

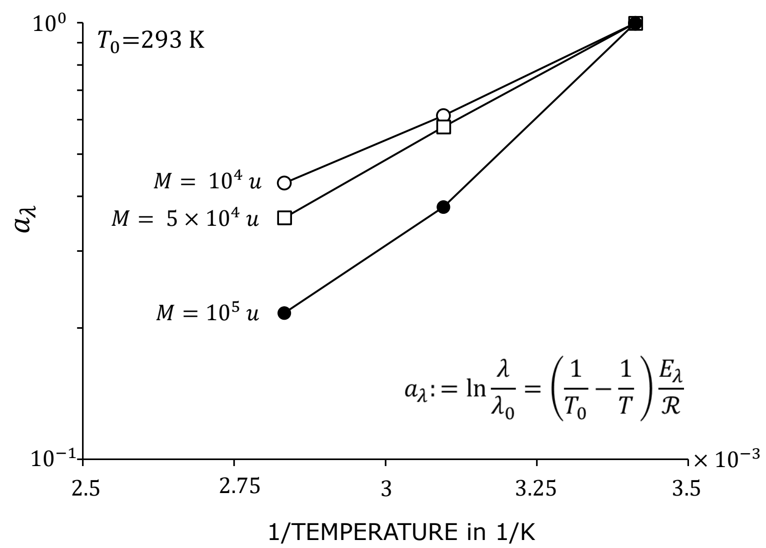

Figure 10. Arrhenius plot for relaxation time of silicone oil molecule in various molecular masses.

4. Simulation

This section investigates the effect of different parameters on the generic gap. Since numerous two-dimensional and three-dimensional simulations have been performed on screw pumps, this work has focused only on the geometry of the generic gap and its parameters. Figure 11 shows the dimensionless ϖ values in different pressures for the Carreau and Maxwell models. Using measurement data in figure 9, it has been shown that the Carreau model does not have high accuracy in high shear rates. For low molecular masses of 10,000 u, the leakage values are close together for these two models. With increasing molecular mass, the difference in values between the two methods is very large. In figure 11, the difference in the leakage values is shown for the two models. The Carreau model calculated higher leakage values for the higher pressure difference parameter. Here, the power-law index of the Carreau model is equal to 0.3.

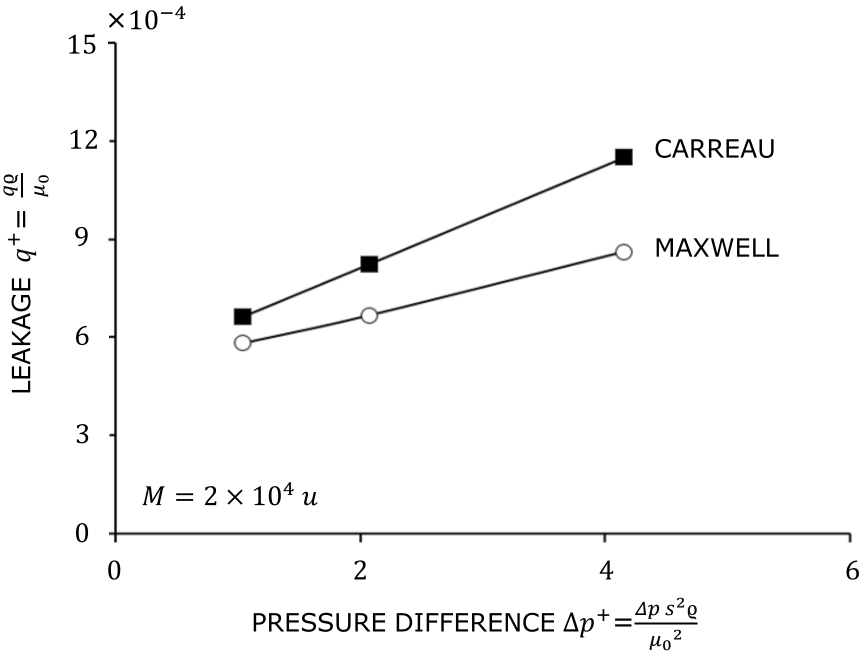

Figure 11. Comparison of dimensionless leakage for Maxwell and Carreau in different pressures

Figure 12 shows velocity values in the generic gap for two different gap angles. The gap angle α was described in figure 2. At low-pressure differences, reducing the gap inlet angle reduces leakage. But this effect changes with increasing viscosity and relaxation time of the molecule. Therefore, a general diagram and conclusion have not been provided here. As can be seen in figure 12, the velocity of the outlet of the gap has decreased as the angle decreases. Hence, we can state that the leakage increased with increasing the gap inlet angle.

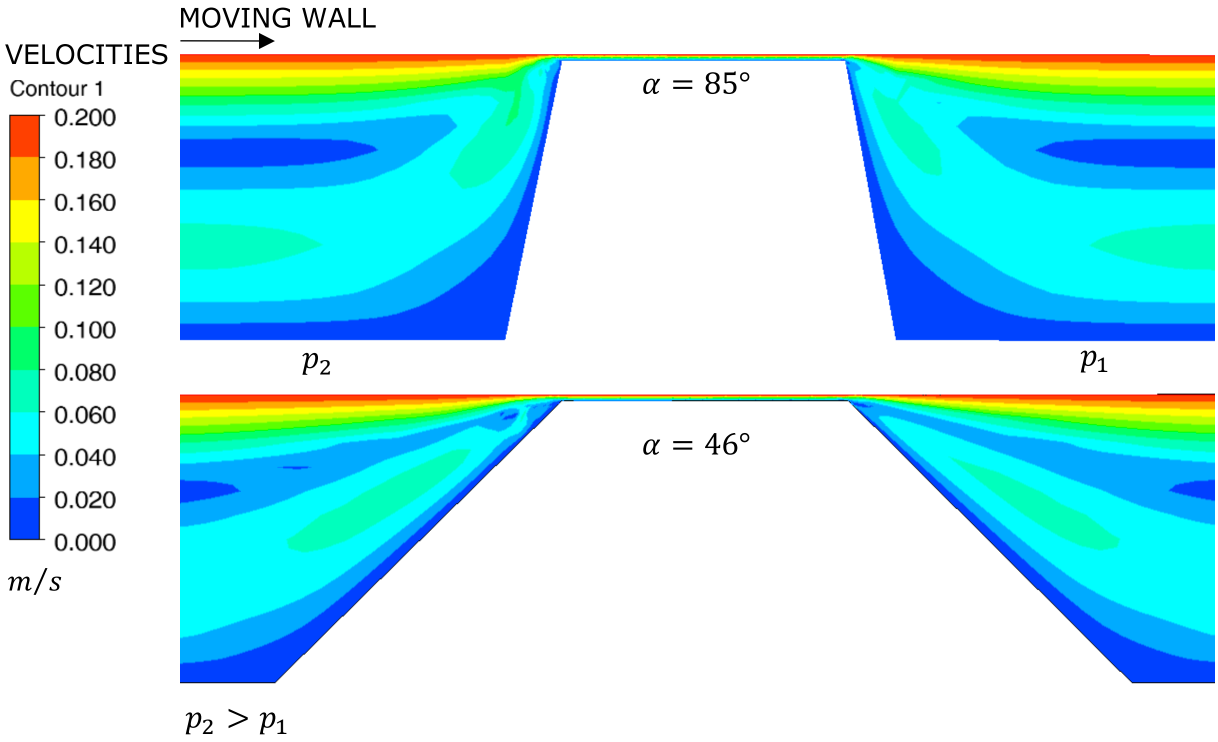

Figure 12. Velocity values in the generic gap for two different gap angles (s/l= 0.02, M= 20,000 $\boldsymbol{u}$, Δp = 20 kPa)

Figure 13 shows dimensionless pressure values across the gap for different Deborah numbers. As it is shown in the figure, with increasing the Deborah number, the pressure drop decreased. In order to explore the reasons, Bagley pressure and elastic loss were studied. Pressure losses versus different gap lengths have shown in figure 14. The Bagley plot supports the separation of the viscose pressure drop and the inlet pressure drop. To determine the inlet pressure drop, the pressure drop is applied with various length ratios of the same gap height but different lengths and extrapolated to zero. Contraction flow at the gap entrance region causes an extra pressure drop due to the stretching of fluid elements. In principle, the significance of the entrance pressure drop compared to the pressure drop across the gap decreases with increasing l/s or relative gap length. The large relative gap length, however, can lead to other errors; the longer the gap is, the greater the pressure effect becomes.
In this graph, the pressure drop is increased with the increasing shear rate. This pressure drop is due to inertia and elastic loss across the gap. For calculating the elastic pressure drop, which depends on the viscosity and relaxation time of fluid, the inertia loss or Carnot loss was calculated and then subtracted from the Bagley pressure drop. For a non-Newtonian fluid, the Carnot loss is negligible compared to the elastic pressure loss. Figure 15 has shown the calculated values of elastic pressure loss at different shear rates. With increasing the shear rate, the values of elastic pressure drop also increased.

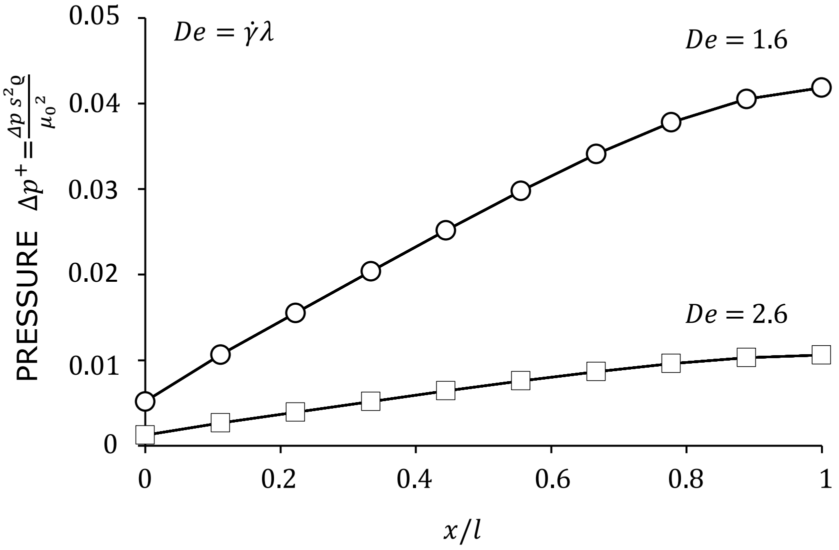

Figure 13. Dimensionless pressure values across the gap for different Deborah numbers.

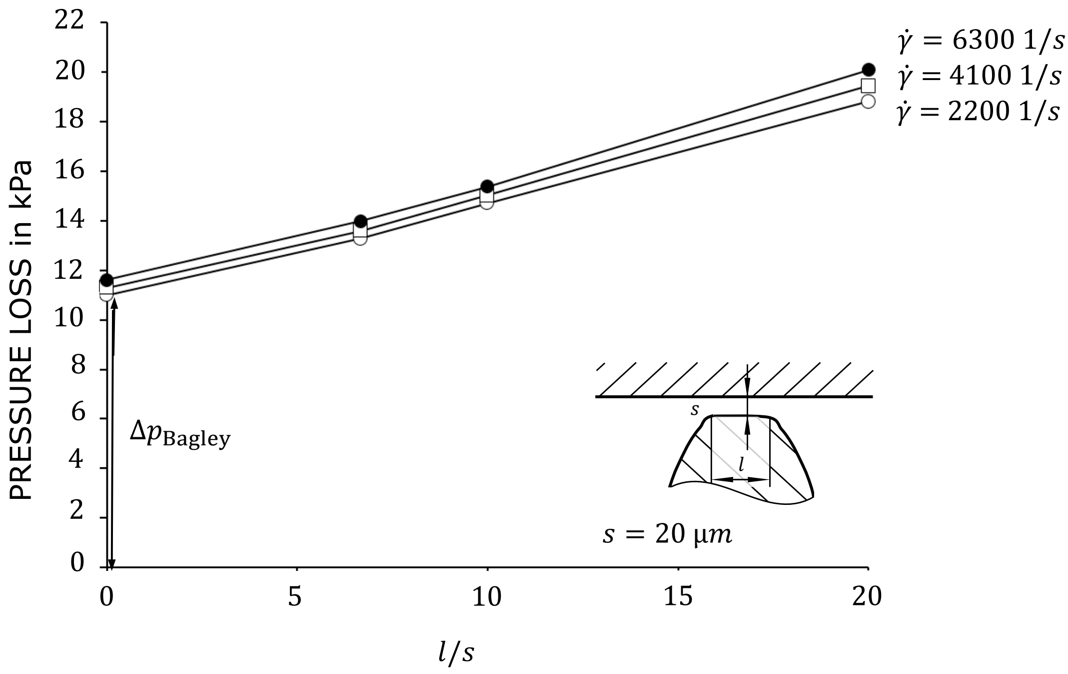

Figure 14. Pressure loss of inflow versus different gap lengths.

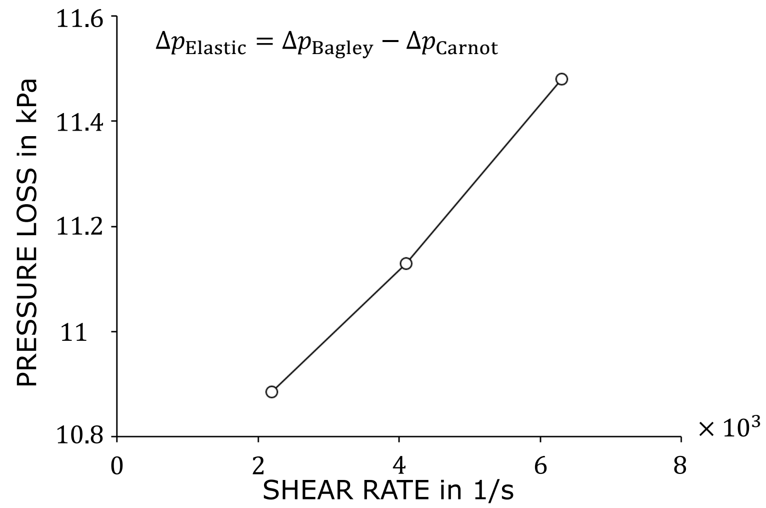

Figure 15. Elastic pressure loss versus shear rate.

Figure 16 shows leakage values versus pressure differences in various slenderness ratios. In this figure, the slenderness ratio s/l is equal to gap height to gap length. As can be seen in this graph, the leakage increases with increasing the slenderness ratio. Also, increasing the pressure increases the leakage.

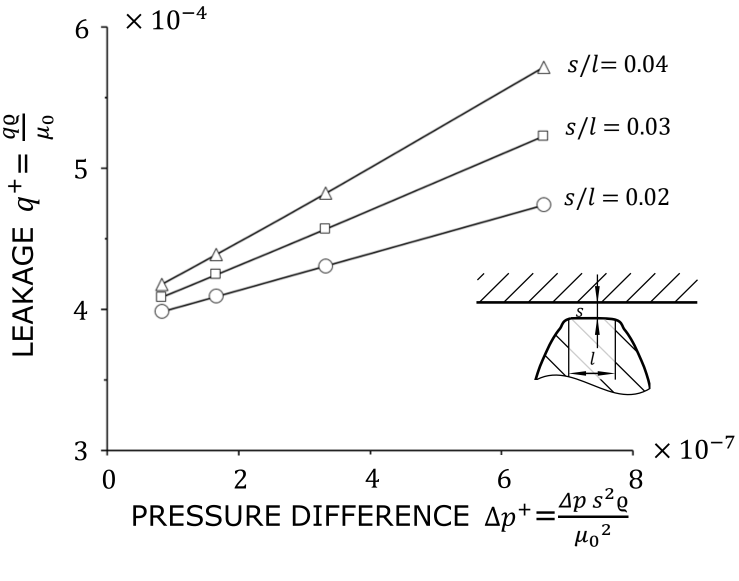

Figure 16. Leakage values versus pressure differences in different slenderness ratios.

5. Conclusion

In the present article, the leakage flow in the generic gap between a stationary wall and a moving wall was investigated numerically by a CFD tool designed for viscoelastic fluid dynamics problems to find the relationship between leakage flow, gap length, and pressure difference. For solving the incompressible, viscous flow field of the continuous phase, the equations for mass and momentum conservation were solved. Also, the flow was assumed to be steady, and the temperature was constant. The non-Newtonian and viscoelastic fluid was modelled by a Maxwell constitutive equation.

Several simplified models used in simulations are the more fitting method, like Carreau. Other viscoelastic fluid models like the Maxwell model, called differential viscoelastic models, have the locality property. Maxwell's model represents the physical characteristics that are equivalent to a damper and a spring in series, which can accurately define the stress relaxation phenomenon. The equation of Maxwell is simple, however, this model is complicated from a computational point of view. A comparison of the viscosity of measurement data with different viscoelastic models shows that Maxwell has the best behaviour for viscosity prediction. It should be noticed, with changing the power-law index, could be had a different fitting for the Carreau model.
The simulation results showed that at low pressures, reducing the gap inlet angle reduces leakage. But this effect was unknown with increasing viscosity and relaxation time of the molecule. The Bagley plot supports the separation of the viscose pressure drop and the inlet pressure drop. To determine the inlet pressure drop, the pressure drop is applied with various length ratios of the same gap height but different lengths and extrapolated to zero. The large relative gap length, however, can lead to other errors; the longer the gap is, the greater the pressure effect becomes. This pressure drop is due to inertia and elastic loss across the gap. For a non-Newtonian fluid, the Carnot loss is negligible compared to the elastic pressure loss. Results showed that with increasing the shear rate, the values of elastic pressure drop also increased. Besides, the leakage increases with increasing the slenderness ratio. We can state with increasing the gap length, the leakage flow rate decreases. In summary, we could conclude:

- The Maxwell model is recommended for use in high molecular masses, however, its computational cost is extremely high.
- By increasing the gap length, the leakage would decrease.
- At low-pressure differences, reducing the gap inlet angle reduces leakage. However, with increasing viscosity, the effect of angle is not significant.
- Leakage decreases with increasing Deborah number.

Acknowledgements
The presented results were obtained within the research project "Verschleißverhalten bei partikelbeladenen Fluiden und Leckage bei nicht-Newton'schen Fluiden in rotierenden Verdrängerpumpen", FKM no. 7051800, funded by Verband Deutscher Maschinen- und Anlagenbau (VDMA), which we carried out for the trade association Pumps + Systems.

6. References

[1] Rituraj F and Vacca A 2019 Modelling and Validation of Tooth Tip Leakages in Gerotor Pumps *ASME-JSME-KSME*10.1115/AJKFluids(2019)**553**.
[2] Rituraj F and Vacca A 2020 An Investigation of Tooth Tip Leakages in Gerotor Pumps: Modeling and Experimental Validation *J. of Verification, Validation and Uncertainty Quantification* 5. 10.1115/1.4046295.
[3] Rituraj F and Vacca A 2021 Investigation of flow through curved constrictions for leakage flow modelling in hydraulic gear pumps, *Mechanical Systems and Signal Processing* (2021)**153**.
[4] Türk M and Verhülsdonk B 2006 Gap leakage behaviour of helical vane rotary lobe pumps *J. World Pumps* (2006) **475**.
[5] Nagamura K, Ikej K, and Tutulan F G 2004 Design and performance of gear pumps with a non-involute tooth profile *Proceedings of the Institution of Mechanical Engineers, Part B: Journal of Engineering Manufacture* **218**(2004)699-711.
[6] Wahab A 2009 Analytical Prediction Technique for Internal Leakage in an External Gear Pump *Proceedings of the ASME Turbo Expo* **5**(2009)85-92.
[7] Rundo M 2017 Models for Flow Rate Simulation in Gear Pumps: A Review *Energies* 10.1261. 10.3390/en10091261.
[8] Rituraj F and Vacca A 2018 External gear pumps operating with non-Newtonian fluids: Modelling and experimental validation *Mechanical Systems and Signal Processing* (2018)**106**.

[9] Rothstein J P McKinley G H 2001 The axisymmetric contraction–expansion: the role of extensional rheology on vortex growth dynamics and the enhanced pressure drop *J. Non-Newtonian Fluid Mech* **98** (2001)33–63.
[10] Li X K, Luo Y, Qi Y and Zhang R 2011 On non-Newtonian lubrication with the upper convected Maxwell model *Applied Mathematical Modelling* **35**(2011)5 2309-2323.
[11] Andrä R 1982 Torsionsschwingungsdämpfer in viskoelastischen Flüssigkeiten, insbesondere in Flüssigkeiten zweiter Ordnung (Book) Ph.D. thesis an der Hochschule Darmstadt.